# Summer fluxes of methane and carbon dioxide from a pond and floating mat in a continental Canadian peatland

**Magdalena Burger[1,2], Sina Berger[1,2], Ines Spangenberg[1,2] and Christan Blodau[1,2]**

[1] Ecohydrology and Biogeochemistry Group, Institute of Landscape Ecology, University of Münster, Germany

[2] School of Environmental Sciences, University of Guelph, Canada

*Correspondence to*: C. Blodau (christian.blodau@uni-muenster.de)

**Abstract**

Ponds smaller than 10000 $m^2$ likely account for about one third of the global lake perimeter. The release of methane ($CH_4$) and carbon dioxide ($CO_2$) from these ponds is often high and significant on the landscape scale. We measured $CO_2$ and $CH_4$ fluxes in a temperate peatland in southern Ontario, Canada, in summer 2014 along a transect from the open water of a small pond (847 $m^2$) towards the surrounding floating mat (5993 $m^2$) and in a peatland reference area. We used a high-frequency closed chamber technique and distinguished between diffusive and ebullitive $CH_4$ fluxes. $CH_4$ fluxes and $CH_4$ bubble frequency increased from a median of 0.14 (0.00 to 0.43) mmol $m^{-2}$ $h^{-1}$ and 4 events $m^{-2}$ $h^{-1}$ on the open water to a median of 0.80 (0.20 to 14.97) mmol $m^{-2}$ $h^{-1}$ and 168 events $m^{-2}$ $h^{-1}$ on the floating mat. The mat was a summer hot spot of $CH_4$ emissions. Fluxes were one order of magnitude higher than at an adjacent peatland site. During daytime the pond was a net source of $CO_2$ equivalents to the atmosphere amounting to 0.13 (−0.02 to 1.06) g $CO_2$ equivalents $m^{-2}$ $h^{-1}$, whereas the adjacent peatland site acted as a sink of −0.78 (−1.54 to 0.29) g $CO_2$ equivalents $m^{-2}$ $h^{-1}$. The photosynthetic $CO_2$ uptake on the floating mat did not counterbalance the high $CH_4$ emissions, which turned the floating mat into a strong net source of 0.21 (−0.11 to 2.12) g $CO_2$ equivalents $m^{-2}$ $h^{-1}$. This study highlights the large small-scale variability of $CH_4$ fluxes and $CH_4$ bubble frequency at the peatland-pond interface and the importance of the often large ecotone areas surrounding small ponds as a source of greenhouse gases to the atmosphere.

## 1. Introduction

Inland waters play a significant role in the global carbon cycle although covering only 3.7 % of the Earth's land surface (Bastviken et al., 2011; Raymond et al., 2013; Tranvik et al., 2009). They transport and sequester autochthonous and terrestrially derived carbon and are also sources of carbon dioxide ($CO_2$) and methane ($CH_4$) to the atmosphere (Cole et al., 2007; Tranvik et al., 2009). Global estimates of $CO_2$ and $CH_4$ emissions from inland waters have recently been corrected upward to 2.1 Pg C $yr^{-1}$ as $CO_2$ (Raymond et al., 2013) and 0.65 Pg C $yr^{-1}$ as $CH_4$ (Bastviken et al., 2011). Together they are similar to the net carbon uptake by terrestrial ecosystems of $-2.5 \pm 1.3$ Pg C $yr^{-1}$ and to approximately one third of the anthropogenic $CO_2$ emissions (Ciais et al., 2013).

Small aquatic systems may be particularly important in this respect (Downing, 2010). According to high-resolution satellite imagery analyzed by Verpoorter et al. (2014), 77 % of the total 117 million lakes belong to the smallest detectable size category of 2000 to 10000 $m^2$ lake area. These waters only contribute 7 % to the area but 32 % to the total lake perimeter (Verpoorter et al., 2014). Numerous processes were found to proceed faster in small aquatic systems than in larger ones. Sequestration rates of organic carbon (Downing, 2010; Downing et al., 2008), the concentrations of $CH_4$, $CO_2$, and dissolved organic carbon (DOC) in the water column (Bastviken et al., 2004; Juutinen et al., 2009; Kelly et al., 2001; Kortelainen et al., 2006; Xenopoulos et al., 2003), and $CH_4$ and $CO_2$ emissions from the water to the atmosphere increase with decreasing lake size (Juutinen et al., 2009; Kortelainen et al., 2006; Michmerhuizen et al., 1996; Repo et al., 2007).

Small and shallow lakes and ponds are common in flat northern glacial landscapes and abundant in peatland areas, where 20 to 30 % of the world's soil organic carbon is stored (Turunen et al., 2002). $CO_2$ emissions from peatland ponds were reported to be in the same order of magnitude than net uptake of $CO_2$ by the peatland vegetation (Dinsmore et al., 2009; Hamilton et al., 1994). $CH_4$ emissions from open waters generally exceed $CH_4$ fluxes from vegetated areas by a factor 3 to 25 (Hamilton et al., 1994; McLaughlin and Webster, 2014; Trudeau et al., 2013). Small and shallow peatland ponds have been generally found to be particular strong emitters of the gas (McEnroe et al., 2009; Trudeau et al., 2013). Moreover, $CH_4$ and $CO_2$ emissions from open waters can be significant on the landscape scale despite their often small area (Dinsmore et al., 2010; Juutinen et al., 2013). Pelletier et al. (2014) estimated that a pond cover of > 37 % could convert a northern peatland from a carbon sink into a carbon source. Such findings are relevant as Hamilton et al. (1994) and Trudeau et al. (2013) reported a pond cover of 8 to 12 % and 42 % in fens and bogs in northern Canada. The authors suspected a contribution of aquatic $CH_4$ fluxes to landscape $CH_4$ fluxes of 30 % and 79 %, respectively. Very high $CH_4$ emissions have also been reported from a floating mat on a

thermokarst pond and a floating mat within a bog pond (Flessa et al., 2008; Sugimoto and Fujita, 1997). Juutinen et al. (2013) documented highest $CH_4$ fluxes from a wet lawn adjacent to a small fen lake compared to the lake itself and fen lawns farther away from the small lake.

Fluxes of $CH_4$ and $CO_2$ from ponds are controlled by environmental and biotic factors. Atmospheric $CH_4$ fluxes are controlled by microbial production and oxidation of $CH_4$ within peat, sediment and surface water and the diffusive, ebullitive, and plant-mediated transport to the atmosphere (Bastviken et al., 2004; Bridgham et al., 2013; Carmichael et al., 2014). $CO_2$ exchange is driven by the interplay of heterotrophic and autotrophic respiration and by photosynthesis of aquatic macrophytes and algae. Both gas fluxes are linked to the quantity and quality of organic and inorganic carbon supplied from the surrounding catchment (Huttunen et al., 2002; Macrae et al., 2004; Tranvik et al., 2009). They are also related to temperature, wind speed and air pressure (e. g. Trudeau et al., 2013; Varadharajan and Hemond, 2012; Wik et al., 2013). Ebullition appears to be of particular importance for $CH_4$ release to the atmosphere (Walter et al., 2006; Wik et al., 2013) and varies on scales of several tens to hundreds of meters (Bastviken et al., 2004; Wik et al., 2013). Emissions of $CH_4$ emissions are generally lower in the pelagic than in the littoral zone, where plant habitats further influence fluxes (Juutinen et al., 2001; Larmola et al., 2004). On the other hand, Trudeau et al. (2013) found 2.5 to 5 times lower $CH_4$ fluxes at the border of fen pools than in the center of the pools with areas of 60 and 200 $m^2$. Measurements in this study were carried out in a situation where pool size has been historically increasing at the expense of surrounding terrestrial areas.

Despite this progress, knowledge on the temporal and spatial variability of $CH_4$ and $CO_2$ fluxes within small pond systems is limited. We know, for example, little about the $CH_4$ and $CO_2$ exchange of transition zones between ponds and surrounding peatlands, which can be especially important due to the high perimeter to area ratio of small ponds (Verpoorter et al., 2014). It is important to consider the net effect of different microforms of peatlands by taking into account the global warming potentials, as $CH_4$ emissions may easily offset carbon sinks in ponds. To gain more insight into these issues we investigated the summer atmospheric $CO_2$ and $CH_4$ exchange of open water, a floating mat and an adjacent peatland area in a temperate peatland in southern Ontario, Canada. In particular we tested the hypothesis that (I) ebullitive and diffusive $CH_4$ fluxes increase from the open water towards a floating mat surrounding the pond. We examined further the expectation that (II) $CH_4$ and $CO_2$ effluxes from the system increases with temperature and wind speed, and investigated if falling air pressure raises $CH_4$ fluxes. To assess the importance of the pond system for the greenhouse gas balance we calculated the net radiative forcing of the investigated peatland microforms.

## 2 Materials and methods

### 2.1 Study site

Wylde Lake Bog is located in the southeastern part of the Luther Marsh Wildlife Management Area (43°54.667' N, 80°24.022' W) (Fig. 1) at about 490 m above sea level and has an area of approximately 7.8 $km^2$. A 600 cm deep profile analyzed by Givelet et al. (2003) documented clay-rich sediments up to 560 cm depth, gyttja from 560 to 490 cm, fen peat from 490 to approximately 300 cm and bog peat above 300 cm depth. The peatland is dominated by mosses, graminoids, dwarf shrubs and sporadic trees, and a pronounced hummock-hollow-microtopography. Common in the peatland are *Sphagnum magellanicum*, *S. capillifolium*, *Carex disperma* and *Chamaedaphne calyculata* and on the floating mat *S. angustifolium, S. magellanicum* and *Rhynchospora alba*. The plant species composition of the study site is given in the Supplementary Information (Table S1). The vicinity of the pond is characterized by small open and larger treed areas dominated by *Larix laricina* and *Picea mariana*. The pond (Fig. 1) has an area of 847 $m^2$ and a depth of 0.3 to 0.8 m. The interface between the water column and the organic deposits is not clearly delimited but consists of a transition zone with suspended organic material. It likely has changed in size, depth, and shape throughout the last decades. Sandilands (1984) reported that larger, adjacent Wylde Lake shrunk from 0.4 $km^2$ in 1928 to 0.05 $km^2$ in 1984. The floating mat (Fig. 1) surrounding the pond has an area of approx. 5993 $m^2$. Climate is temperate continental with a mean annual air temperature of about 6.7 °C, annual precipitation of 946 mm including 148 mm of snowfall, and an average frost-free period from May 7$^{th}$ to October 6$^{th}$ (1981 to 2010, Fergus Shand Dam, National Climate Data and Information Archive, 2014).

### 2.2 Environmental variables

Air temperature, relative humidity, wind speed, wind direction, photosynthetically active radiation (PAR) and precipitation were recorded at the study site by a HOBO U30 weather station (U30-NRC-SYS-B, Onset) (Supplementary Information, Table S2). Water temperature of the pond and the temperature of the floating mat were also continuously measured. Air pressure was recorded at a distance of 1.1 km from the study site (Supplementary Information, Table S2). In addition we qualitatively observed presence of algae in the pond and occasionally took pictures of the pond and algae.

### 2.3 $CH_4$ and $CO_2$ flux measurements with closed chambers

$CH_4$ and $CO_2$ fluxes of the pond and the floating mat were measured once a week from July 10$^{th}$ to September 29$^{th}$, 2014 between 1 pm ± 1.5 hours and 5 pm ± 1.5 hours using closed

chambers designed according to Drösler (2005). We used a long wooden board floating on air-filled canisters on the pond-end ('floating boardwalk') to do our measurements and to minimize pressure on the ground (Supplementary Information, Fig. S1). The other end was secured at the drier end of the floating mat. The cylindrical, transparent Plexiglas chambers had a basal area of 0.12 $m^2$ and a height of 0.40 m. They were equipped with 2 or 3 fans (Micronel Ventilator D341T012GK-2, BEDEK GmbH) to circulate the air, a photosynthetically active radiation (Photosynthetic Light (PAR) Smart Sensor, S-LIA-M002, Onset ) and an air temperature sensor (RH Smart Sensor, S-THB-M002, Onset; see also Supplementary Information for further information on instrumentation, Table S2). To compensate for air pressure differences, we attached a vent tube, 12 cm long and 7 mm inner diameter, to the chamber (Davidson et al., 2002). Transparent chambers were used to measure net ecosystem exchange (NEE) and cooled with up to 6 ice packs depending on ambient temperature to ensure a temperature change of less than 1°°C during the chamber closure. For the measurements chamber orientation was adjusted to avoid shading of the chamber basal area by the ice packs. Ecosystem respiration (ER) was measured with chambers covered with reflective insolation foil. On the water, chambers were operated with a Styrofoam float (0.80 m × 0.61 m × 0.08 m). The chamber walls extended 10 cm below the water surface as recommended by Soumis et al. (2008). $CH_4$ and $CO_2$ concentrations were quantified with an Ultraportable Greenhouse Gas Analyzer (915-001, Los Gatos Research) at a temporal resolution of 1 s. According to the manufacturer, a single data point has a precision of < 2 ppb for $CH_4$ and < 300 ppb for $CO_2$. Stability of the calibration was checked in March and August 2014. The air was circulated between the chamber and the analyzer through low-density polyethylene tubes of 5 m length with an inner diameter of 2 mm and a water vapor trap. Using this setup it took 36 s until the sampling cell of the analyzer was fully flushed and the concentration had stabilized.

Flux measurements on the open water were carried out in 6 locations with increasing distance of 0.7 m to 4.6 m to the floating mat (Supplementary Information, Table S3). A float with chamber was secured in place by a couple of telescopic poles that were rigidly connected to the floating boardwalk. This way we avoided a drifting of the chamber. On the floating mat the chambers were placed on cylindrical PVC collars with a height of 25 cm. Collars had been inserted into the mat to depths of approximately 15 cm prior to the first measurement. Each sampling day fluxes were measured at least once with the transparent and with the radiation-shielded chamber, for 5 min on the pond and 3 min on the floating mat, by placing the chamber gently as soon as the concentration reading was stable. When $CH_4$ concentrations increased sharply within the first 60 s of the measurement due to $CH_4$ bubble release caused by the positioning of the chamber, the measurement was discarded and repeated. Fluxes were

also quantified at a peatland site in the north-northeast of the pond (Fig. 1) with the same approach, every other week from July 4th until October 1st, 2014, on 12 measuring plots covering hummocks, hollows and lawns. In this area of the peatland, hummocks cover 90 % of the area, hollows 9.8 % and lawns 0.2 % of the area.

Fluxes were calculated based on the gas concentration change in the chamber over time using linear regression and the ideal gas law, mean air temperature inside the chamber and the corresponding half hour mean air pressure. The chamber volume was calculated for each measurement depending on the number of ice packs, immersion depth on the pond and mean vegetation height on the floating mat. The first 40 s after chamber deployment were discarded for flux calculation due to the response time of the concentration measurement. If the slope was not significantly different from 0 (F test, $\alpha = 0.05$), the flux was set to 0. Concentration change over time was only < 3 ppm $CO_2$ and < 0.1 ppm $CH_4$ in 12 % of flux measurements. These measurements resulted in fluxes close to 0 with $R^2 < 0.8$. Following Repo et al. (2007), we included them in the data set because their exclusion would have biased the results by increasing the median diffusive fluxes by 52 % ($CO_2$) and 12 % ($CH_4$).

Due to the high temporal resolution of concentration measurements, we were able to quantify $CH_4$ fluxes with and without bubbles. When the $CH_4$ concentrations evolved linearly with a constant slope we used linear regression over the entire time of sampling; when the initial concentration trend was interrupted by one or several sharp increases in slope, followed by a return to the initial slope (Supplementary Information, Fig. S1), we used piecewise linear fitting for each of the linear segments (Goodrich et al., 2011). According to Goodrich et al. (2011) and Xiao et al. (2014), we define sharp increases in slope as ebullitive $CH_4$ fluxes and all others as diffusive or continuous flux of micro-bubbles. Time-weighted averages including diffusive and ebullitive flux segments were calculated. We also computed the $CH_4$ bubble frequency in events $m^{-2}$ $h^{-1}$ as the number of bubble events divided by measuring time and area. In order to evaluate the contribution of ebullitive $CH_4$ flux to the total $CH_4$ flux, the $CH_4$ release of each event in µmol was calculated by multiplying the ebullitive flux with the duration of the event and the basal area of the chamber.

For comparisons of NEE between sites and with time, we used the maximum NEE defined as light-saturated at PAR levels > 1000 µmol $m^{-2}$ $s^{-1}$ according to a study by Larmola et al. (2013). We further calculated the net exchange of $CO_2$ equivalents for each flux measurement. To this end, the $CH_4$ flux was converted into $CO_2$ equivalents by multiplying the mass flux with the global warming potential of 28 for a 100 year time horizon (Myhre et al., 2013). Subsequently, the $CH_4$ flux in $CO_2$ equivalents and the maximum NEE were summed up.

## 2.4 $CO_2$ concentration measurements and gradient flux calculations

To obtain estimates of daily time series of $CO_2$ concentration and fluxes, concentrations of $CO_2$ in the surface water of the pond and in the air were measured with calibrated non-dispersive infrared absorption sensors (CARBOCAB, GMP222, Vaisala) in the range up to 10000 ppm and with an accuracy of ± 150 ppm plus 2 % of the reading. The probe was enclosed in $CO_2$ permeable silicone tubes, as already used by Estop et al. (2012) in peats, and attached to a floating platform at a depth of approximately 18 cm and a distance of 3.2 m from the pond margin. In water equilibration time to 90% of dissolved concentration was approximately one hour when concentration increased but more delayed when it fell (Supplementary Information, Fig. S3). The platform also carried the data logger (MI70, Vaisala). Another silicon-covered sensor measured air $CO_2$ concentrations at 0.3 m above the water surface. Concentration was recorded every 15 min and $CO_2$ flux across the air-water interface estimated according to the boundary layer equation approach (Supplementary Information). Due to frequent failures of the sensors with increased humidity in the sensor head and overheating of the data logger, $CO_2$ fluxes were only calculated for 5 and 3 exemplary days in July and September, respectively. During these periods sensor functioning was stable.

## 2.5 $CH_4$ and $CO_2$ concentrations and diffusive fluxes in the sediment

Dissolved $CH_4$ and $CO_2$ concentrations at the sediment-water-interface were determined with pore water peepers of 60 cm length and 1 cm resolution as developed by Hesslein (1976). The chambers were filled with deionized water, covered with a nylon membrane of 0.2 µm pore size, installed at four locations randomly distributed across the pond on August 21$^{st}$, 2014 and sampled on September 25$^{th}$ and 29$^{th}$, 2014. The pH of every other cell was measured in the field and a sample of 0.5 mL from each chamber filled into a vial containing 20 µL of 4 M hydrochloric acid (HCl). $CO_2$ and $CH_4$ concentrations in the headspace of the vials were determined with an SRI 8610C gas chromatograph equipped with a methanizer and a flame ionization detector on the day after sampling. The original $CO_2$ and $CH_4$ concentrations in the pore water were calculated by using the measured headspace concentrations, Henry's law with temperature corrected Henry's law constants (Sander, 1999) and the ideal gas law. Diffusive fluxes of $CO_2$ and $CH_4$ towards the sediment-water interface were calculated with Fick's first law and diffusion coefficients in water $D_w$ corrected for an assumed sediment temperature of 15°C ($CH_4$: $1.67 \bullet 10^{-5}$ $cm^2$ $s^{-1}$; $CO_2$: $1.87 \bullet 10^{-5}$ $cm^2$ $s^{-1}$) and assuming a porosity n of 0.9. The effect of porosity on the sediment diffusion coefficient was accounted for by multiplying $D_w$ with a factor $n^2$ (Lerman, 1978). We further calculated a theoretical temperature- and depth-dependent threshold of bubble formation using Henry's law,

correcting Henry's law constant for a temperature of 15°C, and assuming a partial pressure of $N_2$ in the pore water of 0.8 atm or 0.5 atm. The assumption here is that bubble formation is possible when the partial pressure of $CH_4$ and remaining $N_2$ exceeds atmospheric and water pressure in the anoxic sediment. In addition we sampled occasionally gas bubbles trapped in an algal mat that was present on the pond until August 12th.

### 2.6 Statistical analyses

Statistical analyses were performed with R, version 3.1.2 (R Core Team, 2014). All datasets were checked for normality with the Shapiro-Wilk normality test at a confidence level of $\alpha = 0.05$. To investigate statistical differences of a continuous variable between two or more groups, we used the non-parametric Kruskal-Wallis rank sum test ($\alpha = 0.05$) and if applicable afterwards the multiple comparison test after Kruskal-Wallis ($\alpha = 0.05$) since none of the datasets were normally distributed. For the investigation of relationships between two continuous variables, we used Spearman's rank correlation ($\alpha = 0.05$). Due to visually different dynamics of the gas fluxes from July 10th to August 7th (here called "mid summer") compared to August 15th to September 29th (here called "late summer"), correlations with environmental variables were examined for the whole period as well as the two subperiods.

## 3 Results

### 3.1 Weather and pond conditions

Three distinct periods of weather occurred. From July 10th until September 10th, 2014, air temperatures remained high with a mean (± standard deviation) of 17.0 ± 2.7 °C (Fig. 2). Most days were sunny with some passing clouds. From September 11th to September 22nd, 2014, mean air temperature had cooled to 10.2 ± 2.8 °C and the first frost occurred on September 14th (Fig. 2). From September 23rd to 29th, mean air temperature was 13.2 ± 7.6 °C with a high daily amplitude from 3.7 ± 1.3 °C to 24.3 ± 1.5 °C and wind speed was low with a mean of 0.14 ± 0.31 m $s^{-1}$ (Fig. 2). Major storms with maximum wind speeds from 3 to 5.5 m $s^{-1}$ on July 23rd, July 28th, August 12th, September 6th, September 11th and September 21st were accompanied by air pressure decline to lows between 944 and 955 hPa. Often rainfall reached an intensity of 2.8 to 6.2 mm in the chosen 5 min time intervals (Fig. 2).

During the summer an algae mat developed in the pond that impeded water circulation (see Supplementary Information for visuals). This algae mat was irreversibly dissolved with the storm on August 12th. As gas exchange with the atmosphere distinctly differed before and

after this event, we used the storm as a distinction between "mid summer" and "late summer" conditions throughout the analysis.

### 3.2 $CH_4$ and $CO_2$ fluxes over time

$CH_4$ fluxes from the pond were significantly lower in the period from July 10$^{th}$ until August 7$^{th}$ with a median of 0.03 mmol $m^{-2}$ $h^{-1}$ compared to a median of 0.21 mmol $m^{-2}$ $h^{-1}$ from August 15$^{th}$ until September 29$^{th}$ (Kruskal-Wallis test, $p < 0.001$, $n = 159$) (Fig. 3 A). The highest median $CH_4$ flux, highest maximum flux, and largest variability were observed on August 15$^{th}$, after the algal mat had been dissolved on August 12$^{th}$. The bubble frequency varied between 0 and 30 events $m^{-2}$ $h^{-1}$ (Fig. 3 B) and the contribution of the ebullitive to the total $CH_4$ flux between 90 % in mid-July and 0 % in late September (Fig. 3 C). Efflux of $CH_4$ from the floating mat was variable but significantly higher in late summer with a median of 0.80 mmol $m^{-2}$ $h^{-1}$ than in mid summer with a median of 0.22 mmol $m^{-2}$ $h^{-1}$ (Kruskal-Wallis test, $p < 0.001$, $n = 84$) (Fig. 4 A). The bubble frequency on the floating mat ranged from 0 to 80 events $m^{-2}$ $h^{-1}$ and the contribution of ebullition to $CH_4$ flux from 0 to 88 % (Fig. 4 B and C). At the peatland site, $CH_4$ fluxes were similar over time with a median of 0.31 mmol $m^{-2}$ $h^{-1}$ and two very high individual fluxes in September and October (Fig. 5 A). The bubble frequency and contribution of ebullition to $CH_4$ flux ranged from 0 to 5 events $m^{-2}$ $h^{-1}$ and 0 to 54 %, respectively (Fig. 5 B and C).

$CO_2$ fluxes from the pond in mid summer had a median of 0.11 mmol $m^{-2}$ $h^{-1}$ and were also significantly lower than the pond $CO_2$ fluxes in late summer with a median of 1.80 mmol $m^{-2}$ $h^{-1}$ (Kruskal-Wallis test, $p < 0.001$, $n = 159$) (Fig. 3 D). During 24 out of 55 individual measurements before August 15$^{th}$, $CO_2$ exchange across the water-atmosphere interface was absent or $CO_2$ was taken up by the pond between 0 and −0.75 mmol $m^{-2}$ $h^{-1}$. Subsequently $CO_2$ was net emitted. The median daytime ER of the floating mat was 6.77 mmol $m^{-2}$ $h^{-1}$ and the median of the maximum NEE −4.81 mmol $m^{-2}$ $h^{-1}$ (Fig. 4 D). Daytime ER at the peatland site varied between 2.61 to 36.93 mmol $m^{-2}$ $h^{-1}$ with a median of 11.98 mmol $m^{-2}$ $h^{-1}$ and tended to decrease towards fall (Fig. 5 D). The maximum NEE was quite constant from July until September with a median of −16.98 mmol $m^{-2}$ $h^{-1}$.

The gradient method provided similar $CO_2$ fluxes in July and September with a median of 1.99 mmol $m^{-2}$ $h^{-1}$ in July and 2.02 mmol $m^{-2}$ $h^{-1}$ in September (Supplementary Information, Fig. S2). The daily amplitude of fluxes determined with this method was 1.46 to 3.19 mmol $m^{-2}$ $h^{-1}$ in July and 1.41 to 1.86 mmol $m^{-2}$ $h^{-1}$ in September (Supplementary Information Fig. S2). Comparing results of floating chamber and gradient method, in July, when the algal mat on the pond was present, the daytime $CO_2$ fluxes obtained by the gradient method were 14-fold higher than the respective $CO_2$ fluxes measured with the floating chambers (Kruskal-

Wallis test, $p < 0.001$, $n = 189$). In September the results of gradient and chamber method were not significantly different.

### 3.3 $CO_2$ and $CH_4$ concentrations and diffusion in the surface water and sediments

$CO_2$ concentrations of the surface water of the pond were similar during the examined periods in July and September with a mean (± standard deviation) of 114.8 ± 33.1 µmol $L^{-1}$ and 132.0 ± 21.0 µmol $L^{-1}$, respectively (Fig. S2, Supplementary Information). In both periods we observed diurnal cycles of $CO_2$ concentrations covering a mean amplitude of 83.5 ± 16.3 µmol $L^{-1}$ (July) and 62.0 ± 3.1 µmol $L^{-1}$ (September). In the sediments, the mean pH was 4.29 ± 0.11 above the sediment-water interface and increased to 5.37 ± 0.28 at a sediment depth of 40 to 60 cm. $CH_4$ concentrations rose with depth from an average of 10.7 ± 20.4 µmol $L^{-1}$ above the sediment-water interface to 557.3 ± 72.9 µmol $L^{-1}$ at a depth of 40 to 60 cm into the sediment (Fig. 6). The concentration began exceeding theoretical thresholds for bubble formation at depths between 10 to 40 cm and at a partial pressure of $N_2$ of 0.8 atm, but nowhere were concentrations sufficient to form bubbles at 0.5 atm $N_2$ (Fig. 6). The average $CO_2$ concentration at 40 to 60 cm depth was 1548.2 ± 332.5 µmol $L^{-1}$ and one order of magnitude higher than above the sediment-water interface (Fig. 6). Diffusive fluxes towards the surface water were on average 10.5 ± 5.6 µmol $m^{-2}$ $h^{-1}$ ($CH_4$) and 16.9 ± 9.4 µmol $m^{-2}$ $h^{-1}$ ($CO_2$), or 12.0 ± 5.6 µmol $m^{-2}$ $h^{-1}$ ($CH_4$) and 25.8 ± 16.1 µmol $m^{-2}$ $h^{-1}$, depending on where the concentration gradient of pore water peeper C is assigned (Fig. 6). *In situ* production and diffusion from the sediment thus contributed only a small fraction to the $CO_2$ and $CH_4$ flux from the pond. The relative inactivity of the pond sediment was also indicated by the mostly flat and linear concentration increase of both gases with depth near the sediment-water interface.

### 3.4 Spatial pattern of $CH_4$ and $CO_2$ fluxes

Efflux of $CH_4$ increased 6-fold from open water towards the floating mat and was also much higher on the floating mat than at the peatland site (Fig. 7 A). The open water median $CH_4$ flux of plot p1, p2 and p3, farthest away from the floating mat, was 0.12 mmol $m^{-2}$ $h^{-1}$ and significantly lower than from plot p4, p5 and p6 closer to the floating mat with a median of 0.19 mmol $m^{-2}$ $h^{-1}$ (Kruskal-Wallis test, $p < 0.05$, $n = 82$) (Supplementary Information, Table S3). The median $CH_4$ flux of the floating mat was 0.64 mmol $m^{-2}$ $h^{-1}$ and significantly higher than the $CH_4$ flux from the pond (Kruskal-Wallis test, $p < 0.001$, $n = 243$). We observed an increasing frequency of ebullition and a higher contribution to $CH_4$ flux towards the floating mat. On plot p1 only 4 events $m^{-2}$ $h^{-1}$ contributing 5 % occurred, whereas on plot m3 on the floating mat 168 events $m^{-2}$ $h^{-1}$ contributing 78 % were found (Fig. 7 B and C). The $CH_4$ flux

of m3 was significantly higher than of m1 and m2 (Kruskal-Wallis multiple comparison test, $p < 0.05$, $n = 84$).

The frequency of ebullition and the amount of $CH_4$ released by bubble events differed along the transect and in comparison to the peatland site. On the pond, bubble events with a comparatively small $CH_4$ release of 0 to 2.5 µmol were most frequent and occurred 5.4 times $m^{-2}$ $h^{-1}$ (Fig. 8). They also contributed the most to the total $CH_4$ release. Bubble events releasing a larger amount of $CH_4$ were rare. The contribution of ebullition to $CH_4$ release was 27 %. On the floating mat, $CH_4$ release by individual bubble events was highly variable with a maximum of 50 µmol (Fig. 8). Larger bubble events were less frequent than smaller ones. However, medium and larger bubble events contributed most to $CH_4$ release with up to 8 %. The contribution of ebullition to $CH_4$ release was 66 % on the floating mat. In contrast, it was only 20 % in the peatland with a clearly different frequency distribution (Fig. 8). Bubble events occurred over a larger range of release strength than on the pond, but they were less frequent with a total bubble frequency of only 1.3 events $m^{-2}$ $h^{-1}$.

The pond was on average also a net source of $CO_2$ with a median $CO_2$ efflux of 1.16 mmol $m^{-2}$ $h^{-1}$ (Fig. 7 D). On the floating mat, daytime ER ranged from 0.53 to 13.45 mmol $m^{-2}$ $h^{-1}$ and maximum NEE from −11.46 to 0.71 mmol $m^{-2}$ $h^{-1}$ (Fig. 7 D).

### 3.5 Controls on $CH_4$ and $CO_2$ fluxes

$CH_4$ and $CO_2$ fluxes from the pond and ER on the floating mat were significantly negatively, and maximum NEE on the floating mat positively correlated with air, water and mat temperature (Table 1 and 2). We found more negative NEE values at an increasing PAR on the floating mat as well as on the pond. Late summer fluxes of $CO_2$ and $CH_4$ across the water-atmosphere interface were positively correlated with wind speed, whereas the respective mid summer fluxes were negatively correlated (Table 1 and 2).

Total $CH_4$ fluxes from the floating mat and the pond were significantly higher for periods with a decreasing air pressure trend over the last 24 h than for periods with an increasing air pressure trend (Kruskal-Wallis test, $p < 0.05$ and $p < 0.01$, $n = 111$ and $n = 61$). At the floating mat median fluxes during these periods were 0.82 and 0.55 mmol $m^{-2}$ $h^{-1}$ , on the pond 0.13 and and 0.04 mmol $m^{-2}$ $h^{-1}$ (see also Supplementary Information, Fig. S4).

### 3.6 Greenhouse gas exchange of the pond system compared to the surrounding peatland

During our daytime measurements the pond and the floating mat were most frequently significant net sources of $CO_2$ equivalents, whereas the peatland was generally a sink of $CO_2$ equivalents (Fig. 9; Kruskal-Wallis multiple comparison test, $p < 0.001$, $n = 218$). The source strength of $CO_2$ equivalents was largest on the floating mat with a median of 0.21 g $CO_2$

equivalents $m^{-2}$ $h^{-}1$. While the floating mat and peatland site took up $CO_2$ at PAR > 1000 µmol $m^{-2}$ $s^{-1}$, the pond emitted $CO_2$ to the atmosphere during 90 % of measurements (see Figs. 3, 4, 5). When both greenhouse gases were emitted, $CH_4$ contributed 59 ± 20 % to the total emission of $CO_2$ equivalents of the pond.

# 4 Discussion

## 4.1 Spatial pattern of $CH_4$ and $CO_2$ fluxes along the peatland – pond ecotone

The peatland and especially the floating mat were summer hot spots of $CH_4$ emissions compared to a variety of sites in other northern peatlands. Fluxes exceeded most, but not all, emissions reported by Hamilton et al. (1994), Strack et al. (2006), Dinsmore et al. (2009), Moore et al. (2011), and Trudeau et al. (2013) from similar environments by an order of magnitude (see also Supplementary Information for a compilation of flux values, Tables S4-S6). On a per-day and mass basis mean fluxes reached 204 and 437 mg $CH_4$-C $m^{-2}$ $d^{-1}$, which is at the high end of fluxes reported in meta-analyses (Olefeldt et al., 2013). Average $CH_4$ emissions from the open water were still substantial at 63 mg $CH_4$-C $m^{-2}$ $d^{-1}$, which is about 5 times the flux reported from the multi-year study of Stordalen Mire in Northern Sweden (Wik et al., 2013). Emissions fell, however, well into the range of fluxes reported from other peatland ponds (Huttunen et al., 2002; Trudeau et al., 2013; Pelletier et al., 2014). In contrast, $CO_2$ fluxes were fairly inconspicuous compared to fluxes in similar systems; on a per-day and mass basis mean maximum NEE reached −5.4 g $CO_2$-C $m^{-2}$ $d^{-1}$ in the bog and −1.27 g $CO_2$-C $m^{-2}$ $d^{-1}$ on the floating mat, and daytime ER 3.91 g $CO_2$-C $m^{-2}$ $d^{-1}$ and 1.85 g $CO_2$-C $m^{-2}$ $d^{-1}$, respectively. The pond on average emitted 0.38 g $CO_2$-C $m^{-2}$ $d^{-1}$. Both pond and floating mat thus lost more $CO_2$ than they fixed during the day, which suggests that in both environments additional $CO_2$ was released, for example stemming from carbon-rich groundwater seeping into the pond.

Part of the surprising source strength of methane can be attributed to the inclusion of ebullition by means of high frequency chamber measurements, similarly as first reported by Goodrich et al. (2011). Fluxes that are visibly affected by ebullition events have often been discarded from static chamber fluxes in the past because the non-linearity of concentration increase over time is problematic when few samples are analyzed by gas chromatography. Ebullition contributed on average 66 % to the emissions on the floating mat and reached 78 % at the plot with the highest methane flux (Figs. 4 and 7). The importance and variability of ebullition was similar as reported from an ombrotrophic peatland in Japan (50 to 64 %; Tokida et al., 2007). The $CH_4$ released by individual bubble events from the floating mat was

also on the same order of magnitude as bubble $CH_4$ release in Sallie's Fen (Goodrich et al., 2011). At that site the bubble frequency of 35 ± 16 events $m^{-2}$ $h^{-1}$ was, however, lower than on the floating mat at Wylde Lake Bog with 54 to 168 events $m^{-2}$ $h^{-1}$. In contrast to these findings, ebullition accounted on average only for 20 % of fluxes at our bog site and 27 % in the pond (Figs. 3 and 5), where bubble frequency of outer plots was less than 9 events $m^{-2}$ $h^{-1}$ and dropped to zero by the end September (Fig. 3). In the pond ebullition was thus less important than reported previously in 11 lakes in Wisconsin (40 to 60 %; Bastviken et al., 2004) and two productive, urban ponds in Sweden and China (> 90 %; Natchimuthu et al., 2014; Xiao et al., 2014).

Even though bubbles were rarely observed on p1, p2 and p3 farther away from the floating mat (Fig. 7) and ceased altogether in September (Fig. 3), formation of $CH_4$ bubbles may have initially been possible in the pond sediments. Concentrations exceeded the threshold concentration of bubble formation at a $N_2$ partial pressure of 0.8 atm in all locations sampled (Fig. 6). Such concentrations were only reached at larger sediment depth, though, and ongoing stripping of $N_2$ with ebullition may have raised concentration thresholds over time (Fechner-Levy and Hemond, 1996). At a remaining $N_2$ partial pressure of 0.5 atm, ebullition was not possible from a theoretical point of view, which may explain its limited importance in the pond. The lack of ebullition later on may have been assisted by falling temperatures in autumn; a change from 20°C to 10°C, for example, raises the threshold for ebullition by 70 µmol $L^{-1}$. Flat or linearly increasing concentration profiles near the sediment-water interface (Fig. 6) also indicated a lack of active production of the gas in this zone. Concentrations of $CH_4$ and $CO_2$ remained low, typically less than 650 and 1500 µmol $L^{-1}$, respectively, suggesting that microbial activity in the sediments was limited. Also the diffusive fluxes were small in units of mass, about 3.5 mg $CH_4$-C $m^{-2}$ $d^{-1}$ and 7.5 mg $CO_2$-C $m^{-2}$ $d^{-1}$, respectively. The continuous emission of $CH_4$ and $CO_2$ from the pond, on average 63 mg $CH_4$-C $m^{-2}$ $d^{-1}$ and 380 mg $CO_2$-C $m^{-2}$ $d^{-1}$, was hence likely driven by respiration in the water column and by advective inflow of groundwater rich in $CH_4$ and $CO_2$.

Our results further suggest that medium and infrequent large bubble events contributed a substantial fraction to the total $CH_4$ flux at the floating mat but not in the bog and the pond (Fig. 8). This was the case even though small bubble events were much more frequent than large ones (Fig. 8). DelSontro et al. (2015) also reported a strong positive correlation between ebullition flux and bubble volume in open water and found that the largest 10 % of the bubbles observed in Lake Wohlen, Switzerland, accounted for 65 % of the $CH_4$ transport. According to the authors, large bubbles are disproportionately important because they contain exponentially more $CH_4$ with increasing diameter, rise faster, and have less time and a

relatively smaller surface area to dissolve or exchange $CH_4$ with the surroundings (DelSontro et al., 2015).

The decline of $CH_4$ fluxes, $CH_4$ bubble frequency and contribution of ebullition from the floating mat to the open water was striking and fluxes were also considerably higher than at the peatland site (Fig. 7). These findings emphasize that the floating mats and transition zones to the open water need to be included when quantifying greenhouse gas budgets of pond and peatland ecosystems. We cannot mechanistically identify the causes for the observed pattern. It seems likely that the peak emissions from the floating mat were caused by an optimum of wet conditions in the peat, favoring methanogenesis and impeding methane oxidation, presence of some *Carex aquatilis* providing for conduit transport of the gas, and potentially by a release of methane from groundwater entering the land-water interface. $CH_4$ flux through plants with aerenchymatic tissues can be responsible for 50 to 97 % of the total $CH_4$ flux in peatlands because the aerenchyma link the anaerobic zone of $CH_4$ production with the atmosphere (Kelker and Chanton, 1997; Kutzbach et al., 2004; Shannon et al., 1996). Kutzbach et al. (2004) found a strong positive correlation between the density of *C. aquatilis* culms and $CH_4$ fluxes, as well as a contribution of 66 ± 20 % of the plant-mediated $CH_4$ flux through *C. aquatilis* to the total flux in wet polygonal tundra. Since ebullition dominated the $CH_4$ flux from the floating mat (Fig. 4) in our particular case this transport mechanism seemed to be of more limited importance, though. Also recently fixed substrates may have played a role for high $CH_4$ emissions from the floating mat. Several studies have found a positive correlation between the rate of photosynthesis and $CH_4$ emissions (Joabsson and Christensen, 2001; Ström et al., 2003), which has been explained by the quick allocation of assimilated labile carbon to the roots and subsequent exudation to the anaerobic rhizosphere (Dorodnikov et al., 2011). These recent photosynthates serve as a preferential source of $CH_4$ compared to older more recalcitrant organic matter (Chanton et al., 1995). Labile organic matter produced by vascular plants was probably also imported from the floating mat to the margin of the pond (Repo et al., 2007; Wik et al., 2013). Given the gradual decline of $CH_4$ fluxes along the transect $CH_4$-rich groundwater may also have entered the floating mat and the pond, a process that we did not investigate.

### 4.2 Controls on $CH_4$ and $CO_2$ fluxes

In agreement with earlier work air pressure change influenced methane flux. We observed 1.5- to 3-fold higher $CH_4$ fluxes from the floating mat and the pond during periods of decreasing compared to increasing air pressure (Supplementary Information, Fig. S4), which was very likely caused by increased ebullition (Wik et al., 2013). Decreased atmospheric

pressure results in bubble expansion, which enhances buoyancy force and entails bubble rise (Chen and Slater, 2015).

The negative correlation of water and mat temperature with $CH_4$ and $CO_2$ fluxes from the pond and $CH_4$ flux and ER of the floating mat (Table 1 and 2) was unexpected, as it is consensus that temperature is an important positive control on these fluxes (Pelletier et al., 2014; Roulet et al., 1997; Sachs et al., 2010; Wik et al., 2014). Also the potential effect of wind speed on $CH_4$ and $CO_2$ fluxes from the pond was ambiguous. Increasing wind speeds should stimulate the exchange of dissolved gases by increasing turbulence of both air and water close to the interface (Crusius and Wanninkhof, 2003). Before August 15$^{th}$, wind speed and $CH_4$ and $CO_2$ efflux from the pond were, however, negatively correlated, whereas the correlation was positive thereafter despite quite consistent wind speed patterns and surface water $CO_2$ concentrations throughout the whole study period (Figs. 2 and S2, Supplementary Information).

Both phenomena may be explained by internal biological processes, i.e. the growth and decay of a dense algal mat on the pond, changing hydrological connection between the pond system and the surrounding peatland, and the influence of the vascular vegetation on the floating mat. The algal mat developed in the beginning of July and was largely irreversibly dissolved by a storm on August 12$^{th}$ (Figs. S5 and S6). During its presence $CO_2$ emissions from the pond remained low (Fig. 3) and were overestimated by the boundary layer equation approach. Amplitudes of dissolved $CO_2$ concentration were strong and concentration decreased with increasing PAR (Table 1). Such dynamics reflects a strong autochthonous photosynthetic and respiratory activity and lack of water mixing. The empirical relationship between $CO_2$ concentration gradient, wind speed and flux, which is largely controlled by turbulence in the water column, obviously did not apply under such conditions. The subsequent shift to high $CO_2$ and $CH_4$ emissions was probably partly caused by the decomposition of the remains of the algal mat, similarly as reported from a boreal and a subtropical pond (Hamilton et al., 1994; Xiao et al., 2014). Other than that, the algal mat probably represented a physical barrier to diffusive and ebullitive gas exchange between water column and atmosphere. We observed trapped gas bubbles within the algal mat with $CH_4$ concentration of only 4 to 8 %; part of the originally contained $CH_4$ may have been re-dissolved and oxidized. Even in shallow lakes and ponds, $CO_2$ and $CH_4$ concentrations can be several-fold higher in the deep water compared to the surface water during certain periods (Dinsmore et al., 2009; Ford et al., 2002). We can only assume that such concentration gradients established in or under the algal mat. Its destruction, mixing of the water column and resuspension of the upper sediment layer probably entailed the observed peak diffusive $CO_2$ and $CH_4$ emissions after the storm on August 12$^{th}$ (Fig. 2, Fig. 3).

### 4.3 Relevance of greenhouse gas emissions from the pond system

In terms of radiative forcing, the floating mat and open water behaved differently than the peatland site during our daytime flux measurements at PAR > 1000 µmol $m^{-2}$ $s^{-1}$. All three bog micro-sites represented daytime sinks of $CO_2$ equivalents and most so the hummocks (Fig. 9), which represented about 90 % of the area. The floating mat and to a lesser extent also the pond were sources of $CO_2$ equivalents to the atmosphere, even at daytime, and had a comparable source strength as the boreal ponds and beaver pond investigated by Hamilton et al. (1994) and Roulet et al. (1997). Net photosynthetic $CO_2$ uptake at light saturation was thus unable to counterbalance the high $CH_4$ emissions of the floating mat in terms of $CO_2$ equivalents; at both the floating mat and the pond emission of $CH_4$ was more important than $CO_2$ exchange in terms of greenhouse gas equivalents. In the pond the average contribution of $CH_4$ was 59 %, which is much higher than reported from a beaver pond at the Mer Bleue bog (5 %; Dinsmore et al., 2009), but comparable to figures from ponds in other studies (36 to 91 %; Hamilton et al., 1994; Huttunen et al., 2002; Pelletier et al., 2014; Repo et al., 2007; Roulet et al., 1997). We ascribe the large differences between the floating mat and the peatland site (Figs. 7 and 10) to the influx of allochthonous organic and inorganic carbon to the pond system from the surroundings and to the different vegetation composition, in particular the occurrence of *Carex aquatilis* on the floating mat, which may have enhanced $CH_4$ production and transport (Kutzbach et al., 2004; Strack et al., 2006). Our results support earlier suggestions that ponds are important for the greenhouse gas budget of peatlands at landscape scale (e.g. Pelletier et al. 2014) and they suggest that changes in the area extent of floating mats and shore length will be an important factor of changes in greenhouse gas budgets with predicted climate change.

## 5 Conclusions

Our summer measurements of atmospheric $CH_4$ and $CO_2$ exchange revealed a substantial small-scale spatial variability with 6- and 42-fold increasing median $CH_4$ fluxes and bubble frequencies, respectively, from the open water of the pond towards the surrounding floating mat. Individual bubble events releasing more than 10 µmol $CH_4$ contributed substantially to summer $CH_4$ emissions from the floating mat, despite their rare occurrence. When $CH_4$ emissions of peatlands that contain ponds are quantified, ebullitive and diffusive $CH_4$ fluxes at the land-water interface hence need to be accounted for and the areal cover of the different microforms and/or plant communities should be thoroughly mapped, as suggested by Sachs et al. (2010) for tundra landscape. We also observed 4- to 16-fold increases in $CH_4$ and $CO_2$

emissions in late summer that were unrelated to meteorological drivers, such as temperature, wind speed and radiation. Hydrological connections to adjacent peatlands and internal hydrological and biological processes, such as the development of algal mats, which can be abundant in small and shallow water bodies (e.g. Dinsmore et al., 2009; Hamilton et al., 1994; Xiao et al., 2014) thus require more attention in the future. During our summer daytime flux measurements, the pond system had a warming effect considering $CH_4$ and $CO_2$ exchange, with the highest net release of $CO_2$ equivalents from the floating mat. We conclude that carbon cycling and hydrology of small ponds and their surrounding ecotone need to be further investigated; these systems are hot spots of greenhouse gas exchange and are likely highly sensitive to anthropogenic climate change due to their shallowness and dependence on water budgets and hydrological processes upstream.

**Acknowledgements**

The study was financially supported by the German Research Foundation (DFG) grant BL 563/21-1 and an international cooperation grant by the German Academic Exchange Service (DAAD) to C. Blodau. We thank C. Wagner-Riddle for the possibility to use the former Blodau laboratory at the School of Environmental Sciences at the University of Guelph and P. Smith and L. Wing for organizational and technical support. We are grateful to M. Neumann from the Grand River Conservation Authority for permission to conduct research in the Luther Marsh Wildlife Management Area, Ontario, Canada, Z. Green for kindly providing satellite images of the study area and C.A. Lacroix (OAC Herbarium, Biodiversity Institute of Ontario) for her friendly help in identifying some plants. We are thankful to M. Goebel for support in the field and advices on study design and data analysis and to Elisa Fleischer for her helpful comments.

**References**

Bastviken, D., Cole, J.J., Pace, M.L., Tranvik, L.J.: Methane emissions from lakes: Dependence of lake characteristics, two regional assessments, and a global estimate. Global Biogeochemical Cycles 18, GB4009, 2004.

Bastviken, D., Tranvik, L.J., Downing, J.A., Crill, P.M., Enrich-Prast, A.: Freshwater Methane Emissions Offset the Continental Carbon Sink. Science 331, 50, 2011.

Bridgham, S.D., Cadillo-Quiroz, H., Keller, J.K., Zhuang, Q.: Methane emissions from wetlands: biogeochemical, microbial, and modeling perspectives from local to global scales. Global Change Biology 19, 1325–1346, 2013.

Carmichael, M.J., Bernhardt, E.S., Bräuer, S.L., Smith, W.K.: The role of vegetation in methane flux to the atmosphere: should vegetation be included as a distinct category in the global methane budget? Biogeochemistry 119, 1–24, 2014.

Chen, X., Slater, L.: Gas bubble transport and emissions for shallow peat from a northern peatland: The role of pressure changes and peat structure. Water Resources Research 51, 151–168, 2015.

Ciais, P., Sabine, C., Bala, G., Bopp, L., Brovkin, V., Canadell, J., Chhabra, A., DeFries, R., Galloway, J., Heimann, M., Jones, C., Le Quéré, C., Myneni, R.B., Piao, S., Thornton, P.: Carbon and Other Biogeochemical Cycles, in: Stocker, T.F., Qin, D., Plattner, G.-K., Tignor, M., Allen, S.K., Boschung, J., Nauels, A., Xia, Y., Bex, V., Midgley, P.M. (Eds.), Climate Change 2013: The Physical Science Basis. Contribution of Working Group I to the Fifth Assessment Report of the Intergovernmental Panel on Climate Change. Cambridge, New York, pp. 465–570, 2013.

Chanton, J.P., Bauer, J.E., Glaser, P.A., Siegel, D.I., Kelley, C.A., Tyler, S.C., Romanowicz, E.H., Lazrus, A..: Radiocarbon evidence for the substrates supporting methane formation within northern Minnesota peatlands. Geochimica et Cosmochimica Acta 59, 3663–3668, 1995.

Cole, J.J., Prairie, Y.T., Caraco, N.F., McDowell, W.H., Tranvik, L.J., Striegl, R.G., Duarte, C.M., Kortelainen, P., Downing, J.A., Middelburg, J.J., Melack, J.: Plumbing the global carbon cycle: Integrating inland waters into the terrestrial carbon budget. Ecosystems 10, 171–184, 2007.

Crusius, J., Wanninkhof, R.: Gas transfer velocities measured at low wind speed over a lake. Limnology and Oceanography 48, 1010–1017, 2003.

Davidson, E.A., Savage, K., Verchot, L. V., Navarro, R.: Minimizing artifacts and biases in chamber-based measurements of soil respiration. Agricultural and Forest Meteorology 113, 21–37, 2002.

DelSontro, T., McGinnis, D.F., Wehrli, B., Ostrovsky, I.: Size Does Matter: Importance of Large Bubbles and Small-Scale Hot Spots for Methane Transport. Environmental Science & Technology 49, 1268–1276, 2015.

Dinsmore, K.J., Billett, M.F., Moore, T.R.: Transfer of carbon dioxide and methane through the soil-water-atmosphere system at Mer Bleue peatland, Canada. Hydrological Processes 23, 330–341, 2009.

Dinsmore, K.J., Billett, M.F., Skiba, U.M., Rees, R.M., Drewer, J., Helfter, C.: Role of the aquatic pathway in the carbon and greenhouse gas budgets of a peatland catchment. Global Change Biology 16, 2750–2762, 2010.

Dorodnikov, M., Knorr, K.H., Kuzyakov, Y., Wilmking, M.: Plant-mediated $CH_4$ transport and contribution of photosynthates to methanogenesis at a boreal mire: A $^{14}C$ pulse-labeling study. Biogeosciences 8, 2365–2375, 2011.

Downing, J.A.: Emerging global role of small lakes and ponds: little things mean a lot. Limnetica 29, 9–24, 2010.

Downing, J.A., Cole, J.J., Middelburg, J.J., Striegl, R.G., Duarte, C.M., Kortelainen, P., Prairie, Y.T., Laube, K.A.: Sediment organic carbon burial in agriculturally eutrophic impoundments over the last century. Global Biogeochemical Cycles 22, GB1018, 2008.

Drösler, M.: Trace gas exchange and climatic relevance of bog ecosystems, Southern Germany. Doctoral thesis, Technical University of Munich, 2005.

Estop-Aragonés, C., Knorr, K.H., Blodau, C. : Controls on in situ oxygen and DIC dynamics in peats of a temperate fen. Journal of Geophysical Research, 117, 2012.

Fechner-Levy, E.J., Hemond, H.F.: Trapped methane volume and potential effects on methane ebullition in a northern peatland. Limnology and Oceanography 41, 1375–1383,1996.

Flessa, H., Rodionov, A., Guggenberger, G., Fuchs, H., Magdon, P., Shibistova, O., Zrazhevskaya, G., Mikheyeva, N., Kasansky, O., Blodau, C.: Landscape controls of $CH_4$ fluxes in a catchment of the forest tundra ecotone in northern Siberia. Global Change Biology 14, 2040–2056, 2008.

Ford, P.W., Boon, P.I., Lee, K.: Methane and oxygen dynamics in a shallow floodplain lake: the significance of periodic stratification. Hydrobiologia 485, 97–110, 2002.

Givelet, N., Roos-Barraclough, F., Shotyk, W.: Predominant anthropogenic sources and rates of atmospheric mercury accumulation in southern Ontario recorded by peat cores from three bogs: comparison with natural "background" values (past 8000 years). Journal of Environmental Monitoring 5, 935–949, 2003.

Goodrich, J.P., Varner, R.K., Frolking, S., Duncan, B.N., Crill, P.M.: High-frequency measurements of methane ebullition over a growing season at a temperate peatland site. Geophysical Research Letters 38, L07404, 2011.

Hamilton, J.D., Kelly, C.A., Rudd, J.W.M., Hesslein, R.H., Roulet, N.T.: Flux to the atmosphere of $CH_4$ and $CO_2$ from wetland ponds on the Hudson Bay lowlands (HBLs). Journal of Geophysical Research 99, 1495–1510, 1994.

Hesslein, R.H.: An in situ sampler for close interval pore water studies. Limnology and Oceanography 21, 912–914, 1976.

Huttunen, J.T., Väisänen, T.S., Heikkinen, M., Hellsten, S., Nykänen, H., Nenonen, O., Martikainen, P.J.: Exchange of $CO_2$, $CH_4$ and $N_2O$ between the atmosphere and two northern boreal ponds with catchments dominated by peatlands or forests. Plant and Soil 242, 137–146, 2002.

Joabsson, A., Christensen, T.R.: Methane emissions from wetlands and their relationship with vascular plants: an Arctic example. Global Change Biology 7, 919–932, 2001.

Juutinen, S., Alm, J., Martikainen, P., Silvola, J.: Effects of spring flood and water level draw-down on methane dynamics in the littoral zone of boreal lakes. Freshwater Biology 46, 855–869, 2001.

Juutinen, S., Rantakari, M., Kortelainen, P.L., Huttunen, J.T., Larmola, T., Alm, J., Silvola, J., Martikainen, P.J.: Methane dynamics in different boreal lake types. Biogeosciences 6, 209–223, 2009.

Juutinen, S., Väliranta, M., Kuutti, V., Laine, a. M., Virtanen, T., Seppä, H., Weckström, J., Tuittila, E.S.: Short-term and long-term carbon dynamics in a northern peatland-stream-lake continuum: A catchment approach. Journal of Geophysical Research: Biogeosciences 118, 171–183, 2013.

Kelker, D., Chanton, J.: The effect of clipping on methane emissions from *Carex*. Biogeochemistry 39, 37–44, 1997.

Kelly, C.A., Fee, E., Ramlal, P.S., Rudd, J.W.M., Hesslein, R.H., Anema, C., Schindler, E.U.: Natural variability of carbon dioxide and net epilimnetic production in the surface waters of boreal lakes of different sizes. Limnology and Oceanography 46, 1054–1064, 2001.

Kortelainen, P.L., Rantakari, M., Huttunen, J.T., Mattsson, T., Alm, J., Juutinen, S., Larmola, T., Silvola, J., Martikainen, P.J.: Sediment respiration and lake trophic state are important predictors of large CO2 evasion from small boreal lakes. Global Change Biology 12, 1554–1567, 2006.

Kutzbach, L., Wagner, D., Pfeiffer, E.M.: Effect of microrelief and vegetation on methane emission from wet polygonal tundra, Lena Delta, Northern Siberia. Biogeochemistry 69, 341–362, 2004.

Larmola, T., Alm, J., Juutinen, S., Huttunen, J.T., Martikainen, P.J., Silvola, J.: Contribution of vegetated littoral zone to winter fluxes of carbon dioxide and methane from boreal lakes. Journal of Geophysical Research: Atmospheres 109, D19102, 2004.

Larmola, T., Bubier, J.L., Kobyljanec, C., Basiliko, N., Juutinen, S., Humphreys, E.R., Preston, M., Moore, T.R.: Vegetation feedbacks of nutrient addition lead to a weaker carbon sink in an ombrotrophic bog. Global Change Biology 19, 3729–3739, 2013.

Lerman A.: Chemical exchange across sediment-water interface. Annual Review of Earth and Planetary Sciences 6, 281-303, 1978.

Macrae, M.L., Bello, R.L., Molot, L.A.: Long-term carbon storage and hydrological control of $CO_2$ exchange in tundra ponds in the Hudson Bay Lowland. Hydrological Processes 18, 2051–2069, 2004.

McEnroe, N.A., Roulet, N.T., Moore, T.R., Garneau, M.: Do pool surface area and depth control $CO_2$ and $CH_4$ fluxes from an ombrotrophic raised bog, James Bay, Canada? Journal of Geophysical Research 114, G01001, 2009

McLaughlin, J., Webster, K.: Effects of Climate Change on Peatlands in the Far North of Ontario, Canada : A Synthesis. Arctic, Antarctic and Alpine Research 46, 84–102, 2014.

Moore, T.R., De Young, A., Bubier, J.L., Humphreys, E.R., Lafleur, P.M., Roulet, N.T.: A Multi-Year Record of Methane Flux at the Mer Bleue Bog, Southern Canada. Ecosystems 14, 646–657, 2011.

Michmerhuizen, C.M., Striegl, R.G., McDonald, M.E.: Potential methane emission from north-temperate lakes following ice melt. Limnology and Oceanography 41, 985–991, 1996.

Myhre, G., Shindell, D., Bréon, F.-M., Collins, W., Fuglestvedt, J., Huang, J., Koch, D., Lamarque, J.-F., Lee, D., Mendoza, B., Nakajima, T., Robock, A., Stephens, G., Takemura, T., Zhang, H.: Anthropogenic and Natural Radiative Forcing, in: Stocker, T.F., Qin, D., Plattner, G.-K., Tignor, M., Allen, S.K., Boschung, J., Nauels, A., Xia, Y., Bex, V., Midgley, P.M. (Eds.), Climate Change 2013: The Physical Science Basis. Contribution of Working Group I to the Fifth Assessment Report of the Intergovernmental Panel on Climate Change. Cambridge, New York, pp. 659–740, 2013.

Natchimuthu, S., Panneer Selvam, B., Bastviken, D.: Influence of weather variables on methane and carbon dioxide flux from a shallow pond. Biogeochemistry 119, 403–413, 2014.

National Climate Data and Information Archive: Canadian Climate Normals. URL http://climate.weather.gc.ca/climate_normals/index_e.html (accessed November 18th, 2014).

Olefeldt, D., Turetsky, M.R., Crill P.M., McGuire, A.D.: Environmental and physical controls on northern terrestrial methane emissions across permafrost zones. Global Change Biology 19, 589-603, 2013.

Pelletier, L., Strachan, I.B., Garneau, M., Roulet, N.T.: Carbon release from boreal peatland open water pools: Implication for the contemporary C exchange. Journal of Geophysical Research: Biogeosciences 119, 207–222, 2014.

R Core Team: R: A language and environment for statistical computing. R Foundation for Statistical Computing, Vienna, 2014.

Raymond, P.A., Hartmann, J., Lauerwald, R., Sobek, S., McDonald, C., Hoover, M., Butman, D., Striegl, R.G., Mayorga, E., Humborg, C., Kortelainen, P.L., Dürr, H., Meybeck, M., Ciais, P., Guth, P.: Global carbon dioxide emissions from inland waters. Nature 503, 355–359, 2013.

Repo, M.E., Huttunen, J.T., Naumov, A. V., Chichulin, A. V., Lapshina, E.D., Bleuten, W., Martikainen, P.J.: Release of $CO_2$ and $CH_4$ from small wetland lakes in western Siberia. Tellus 59B, 788–796, 2007.

Roulet, N.T., Crill, P.M., Comer, N.T., Dove, A., Boubonniere, R.A.: Flux between a boreal beaver pond and the atmosphere. Journal of Geophysical Research 102, 29313–29319, 1997.

Sachs, T., Giebels, M., Boike, J., Kutzbach, L.: Environmental controls on $CH_4$ emission from polygonal tundra on the microsite scale in the Lena river delta, Siberia. Global Change Biology 16, 3096–3110, 2010.

Sander, R.: Compilation of Henry's Law Constants for Inorganic and Organic Species of Potential Importance in Environmental Chemistry. Max-Planck Institute of Chemistry, Mainz, 1999.

Sandilands, A.P.: Annotated Checklist of the Vascular Plants and Vertebrates of Luther Marsh, Ontario. Ontario Field Biologist, Special Publication No. 2. 1984.

Shannon, R.D., White, J.R., Lawson, J.E., Gilmour, B.S.: Methane efflux from emergent vegetation in peatlands. Journal of Ecology 84, 239–246, 1996.

Soumis, N., Canuel, R., Lucotte, M.: Evaluation of two current approaches for the measurement of carbon dioxide diffusive fluxes from lentic ecosystems. Environmental Science and Technology 42, 2964–2969, 2008.

Strack, M., Waller, M.F., Waddington, J.M.: Sedge succession and peatland methane dynamics: A potential feedback to climate change. Ecosystems 9, 278–287, 2006.

Ström, L., Ekberg, A., Mastepanov, M., Christensen, T.R.: The effect of vascular plants on carbon turnover and methane emissions from a tundra wetland. Global Change Biology 9, 1185–1192, 2003.

Sugimoto, A., Fujita, N.: Characteristics of methane emissions from different vegetations on a wetland. Tellus 49B, 382–392, 1997.

Tokida, T., Miyazaki, T., Mizoguchi, M., Nagata, O., Takakai, F., Kagemoto, A., Hatano, R.: Falling atmospheric pressure as a trigger for methane ebullition from peatland. Global Biogeochemical Cycles 21, GB2003, 2007.

Tranvik, L.J., Downing, J.A., Cotner, J.B., Loiselle, S.A., Striegl, R.G., Ballatore, T.J., Dillon, P., Finlay, K., Fortino, K., Knoll, L.B., Kortelainen, P.L., Kutser, T., Larsen, S.,

Laurion, I., Leech, D.M., McCallister, S.L., Mcknight, D.M., Melack, J.M., Overholt, E., Porter, J.A., Prairie, Y.T., Renwick, W.H., Roland, F., Sherman, B.S., Schindler, D.W., Sobek, S., Tremblay, A., Vanni, M.J., Verschoor, A.M., Wachenfeldt, E. Von, Weyhenmeyer, G.A.: Lakes and reservoirs as regulators of carbon cycling and climate. Limnology and Oceanography 54, 2298–2314, 2009.

Trudeau, N.C., Garneau, M., Pelletier, L.: Methane fluxes from a patterned fen of the northeastern part of the La Grande river watershed, James Bay, Canada. Biogeochemistry 113, 409–422, 2013.

Turunen, J., Tomppo, E., Tolonen, K., Reinikainen, A.: Estimating carbon accumulation rates of undrained mires in Finland – application to boreal and subarctic regions. The Holocene 12, 69–80, 2002.

Varadharajan, C., Hemond, H.F.: Time-series analysis of high-resolution ebullition fluxes from a stratified, freshwater lake. Journal of Geophysical Research: Biogeosciences 117, G02004, 2012.

Verpoorter, C., Kutser, T., Seekell, D.A., Tranvik, L.J.: A global inventory of lakes based on high-resolution satellite imagery. Geophysical Research Letters 41, 6396–6402, 2014.

Walter, K.M., Zimov, S.A., Chanton, J.P., Verbyla, D., Chapin, F.S.: Methane bubbling from Siberian thaw lakes as a positive feedback to climate warming. Nature 443, 71–75, 2006.

Wik, M., Crill, P.M., Varner, R.K., Bastviken, D.: Multiyear measurements of ebullitive methane flux from three subarctic lakes. Journal of Geophysical Research: Biogeosciences 118, 1307–1321, 2013.

Wik, M., Thornton, B.F., Bastviken, D., MacIntyre, S., Varner, R.K., Crill, P.M.: Energy input is primary controller of methane bubbling in subarctic lakes. Geophysical Research Letters 41, 555–560, 2014.

Xenopoulos, M.A., Lodge, D.M., Frentress, J., Kreps, T.A., Bridgham, S.D., Grossman, E., Jackson, C.J.: Regional comparisons of watershed determinants of dissolved organic carbon in temperate lakes from the Upper Great Lakes region and selected regions globally. Limnology and Oceanography 48, 2321–2334, 2003.

Xiao, S., Yang, H., Liu, D., Zhang, C., Lei, D., Wang, Y., Peng, F., Li, Y., Wang, C., Li, X., Wu, G., Liu, L.: Gas transfer velocities of methane and carbon dioxide in a subtropical shallow pond. Tellus 66B, 23795, 2014.

Table 1. Correlations of $CH_4$ and $CO_2$ fluxes of the pond with environmental variables. $CH_4$ flux comprises both ebullition and diffusion if not annotated otherwise.

| Flux | Time period | Spearman's rho | P | n |
|---|---|---|---|---|
| *mean air temperature since sunrise* | | | | |
| $CO_2$ | whole period | − 0.54 | < 0.001 | 147 |
| $CH_4$ | whole period | − 0.36 | < 0.001 | 147 |
| diffusive $CH_4$[a] | whole period | − 0.67 | < 0.001 | 119 |
| *mean water temperature during measurements* | | | | |
| $CO_2$ | whole period | − 0.47 | < 0.001 | 94 |
| $CH_4$ | whole period | − 0.50 | < 0.001 | 94 |
| diffusive $CH_4$[a] | whole period | − 0.60 | < 0.001 | 82 |
| *mean PAR of the last 3 h* | | | | |
| $CO_2$ | whole period | − 0.49 | < 0.001 | 147 |
| *mean wind speed of the last 24 h* | | | | |
| $CO_2$ | mid summer[b] | − 0.35 | < 0.05 | 43 |
| $CO_2$ | late summer[c] | + 0.45 | < 0.001 | 104 |
| $CO_2$ | whole period | not significant | | |
| $CH_4$ | mid summer[b] | − 0.35 | < 0.05 | 43 |
| $CH_4$ | late summer[c] | + 0.63 | < 0.001 | 104 |
| $CH_4$ | whole period | + 0.26 | < 0.01 | 147 |
| *maximum wind speed of the last 24 h* | | | | |
| $CO_2$ | mid summer[b] | − 0.45 | < 0.01 | 43 |
| $CO_2$ | late summer[c] | + 0.35 | < 0.001 | 104 |
| $CO_2$ | whole period | + 0.17 | < 0.05 | 147 |
| $CH_4$ | mid summer[b] | − 0.55 | < 0.001 | 43 |
| $CH_4$ | late summer[c] | + 0.63 | < 0.001 | 104 |
| $CH_4$ | whole period | + 0.32 | < 0.001 | 147 |

[a]: only measurements without ebullition included
[b]: July 10th to August 7th
[c]: August 15th to September 29th

Table 2. Correlations of $CH_4$ and $CO_2$ fluxes of the floating mat with environmental variables. $CH_4$ flux comprises both ebullition and diffusion if not annotated otherwise

| Flux | Time period | Spearman's rho | P | n |
|---|---|---|---|---|
| *mean air temperature since sunrise* | | | | |
| max. NEE | whole period | + 0.74 | < 0.001 | 20 |
| $CH_4$ | whole period | − 0.42 | < 0.001 | 79 |
| *mean mat temperature during measurements* | | | | |
| ER | whole period | − 0.44 | < 0.01 | 38 |
| $CH_4$ | whole period | − 0.41 | < 0.001 | 79 |
| diffusive $CH_4$[a] | whole period | − 0.52 | < 0.001 | 53 |
| *mean PAR during measurements* | | | | |
| NEE | mid summer[b] | not significant | | |
| NEE | late summer[c] | − 0.60 | < 0.01 | 26 |
| NEE | whole period | − 0.37 | < 0.05 | 42 |

[a]: only measurements without ebullition included
[b]: July 10th to August 7th
[c]: August 15th to September 29th

## Figures

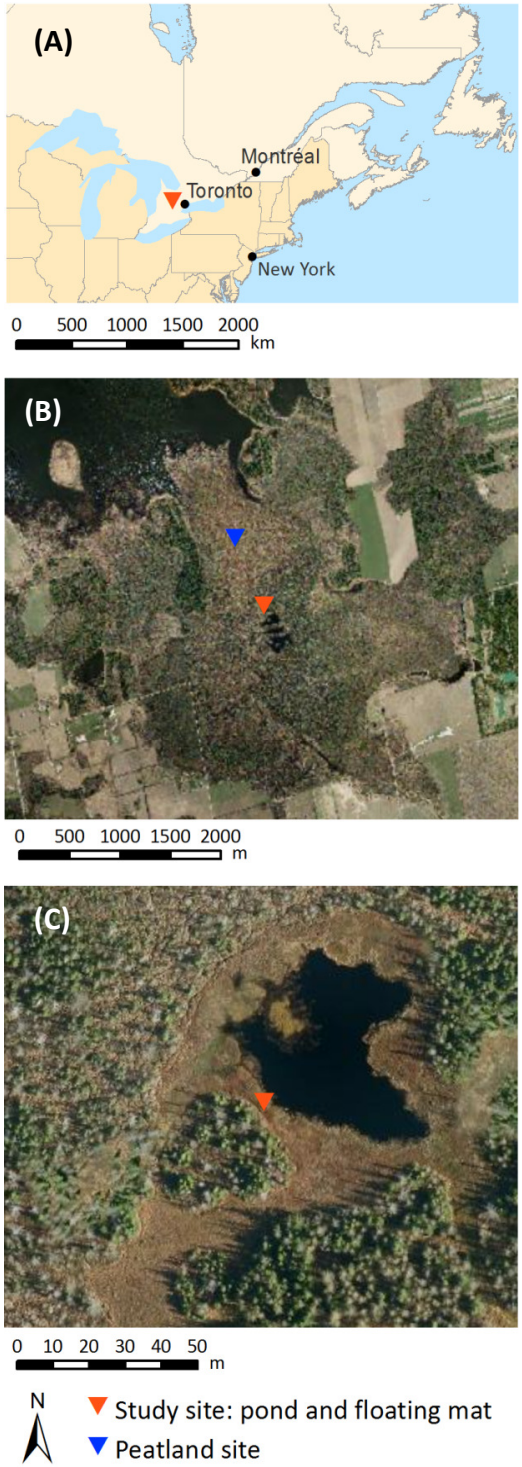


Figure 1. Location of the study site in southern Ontario, Canada (panel A), studied pond with floating mat and peatland site in Wylde Lake Bog in the Luther Marsh Wildlife Management Area with Luther Lake in the northwest (panel B) and close-up of the studied pond and floating mat (panel C) (Grand River Conservation Authority, 2010)

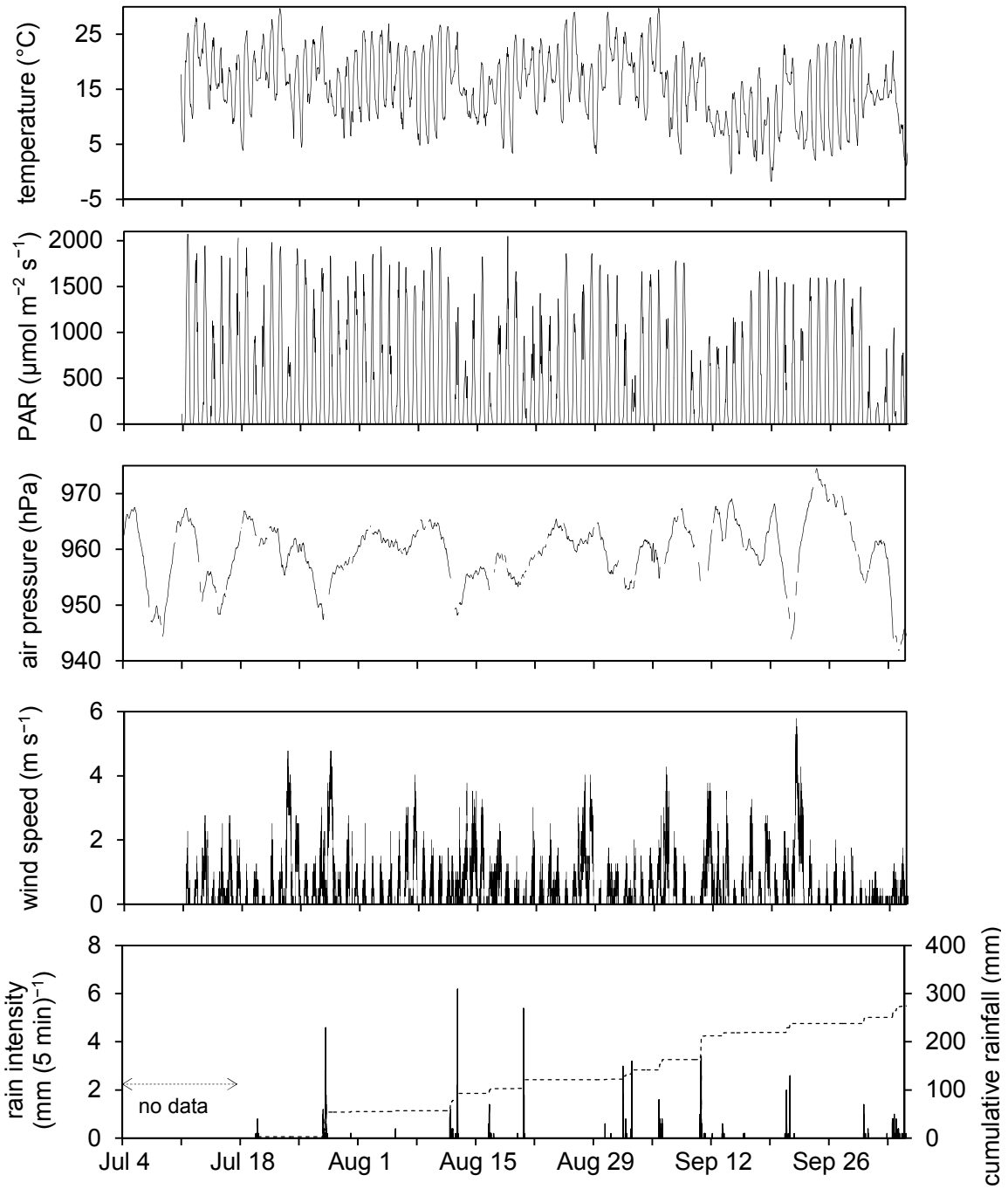


Figure 2. Time series of weather variables at the study site. Air temperature, photosynthetically active radiation (PAR) and air pressure are shown as hourly means, wind speed and rain intensity as 5 min averages. The dashed line in the lowest panel shows the cumulative rainfall.

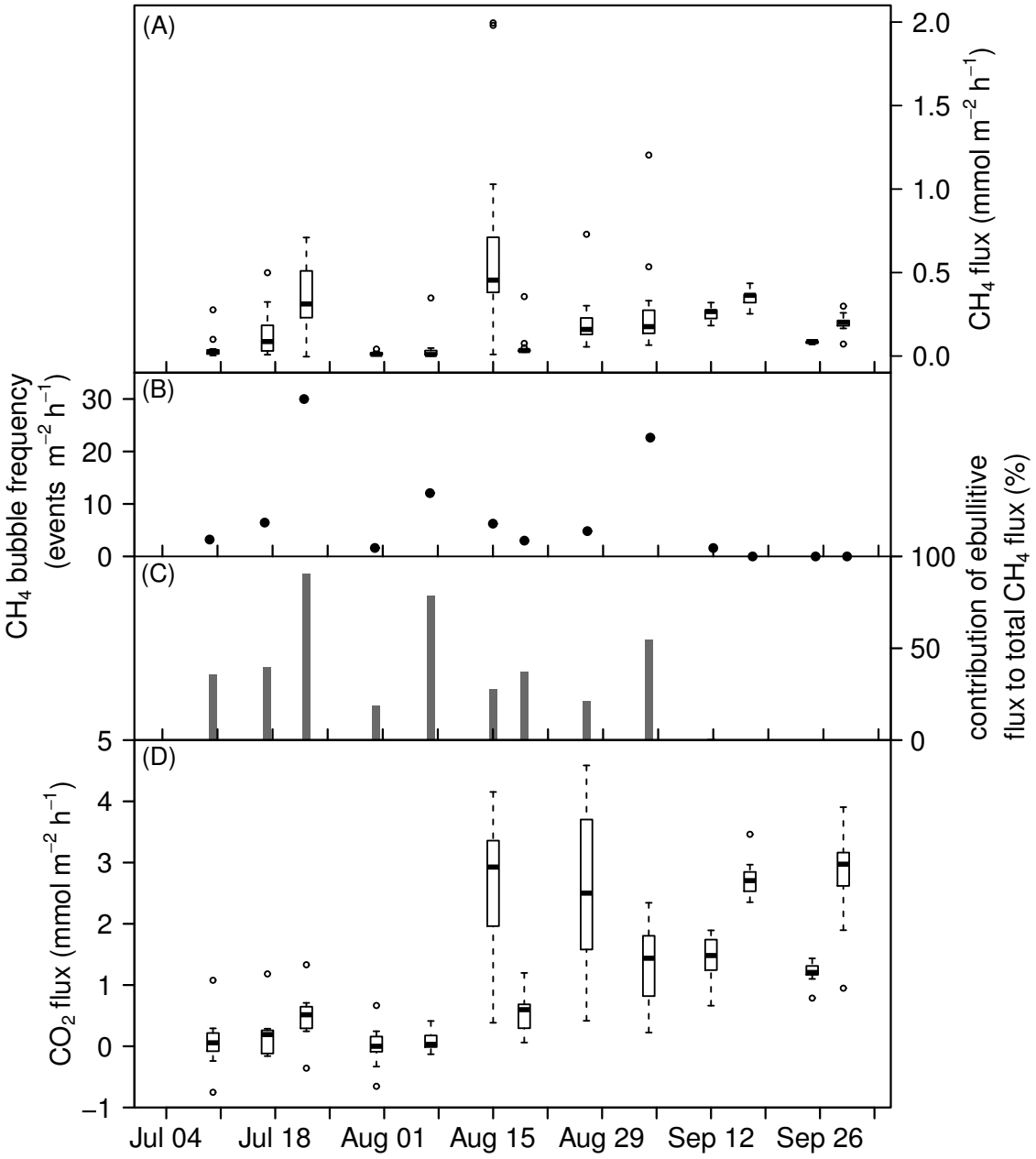


Figure 3. Time series of pond $CH_4$ fluxes (panel A), $CH_4$ bubble frequency (panel B), contribution of ebullitive $CH_4$ flux to total $CH_4$ flux (panel C) and $CO_2$ fluxes (panel D) on measuring days from July 10$^{th}$ until September 29$^{th}$, 2014. In panel (A) and (D), the bold horizontal line shows the median, the bottom and the top of the box the 25$^{th}$ and 75$^{th}$ percentile and the whiskers include all values within 1.5 times the interquartile range.

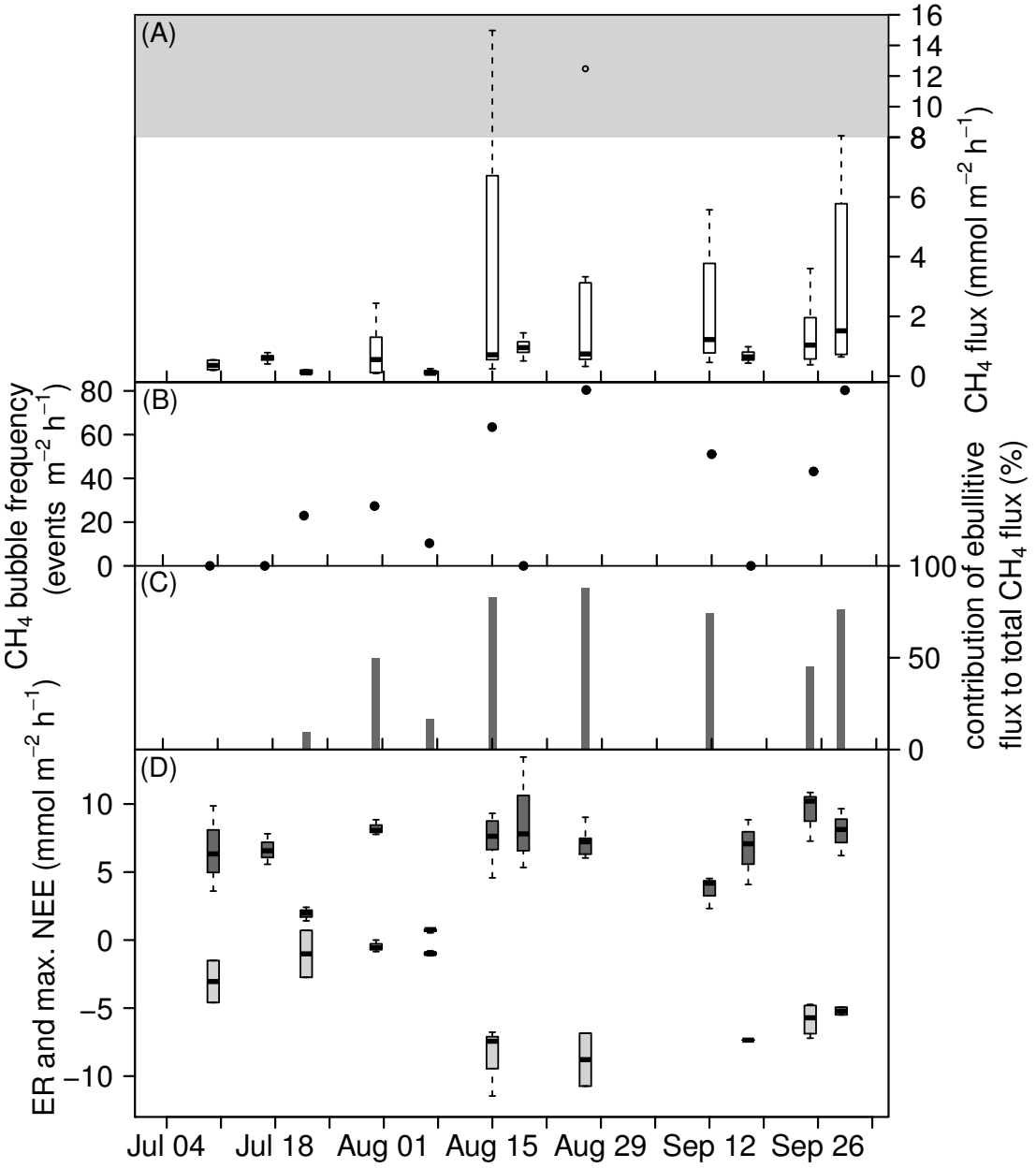


Figure 4. Time series of floating mat $CH_4$ fluxes (panel A), $CH_4$ bubble frequency (panel B), contribution of ebullitive $CH_4$ flux to total $CH_4$ flux (panel C) as well as ecosystem respiration (ER) and maximum net ecosystem exchange (NEE) (panel D) on measuring days from July 10$^{th}$ until September 29$^{th}$, 2014. Note the different scaling of the y-axis within the gray area in panel (A). In panel (D), the dark gray boxes show the daytime ER and the light gray boxes the maximum net ecosystem exchange at values of photosynthetically active radiation > 1000 µmol $m^{-2}$ $s^{-1}$. In panel (A) and (D), the bold horizontal line shows the median, the bottom and the top of the box the 25$^{th}$ and 75$^{th}$ percentile and the whiskers include all values within 1.5 times the interquartile range.

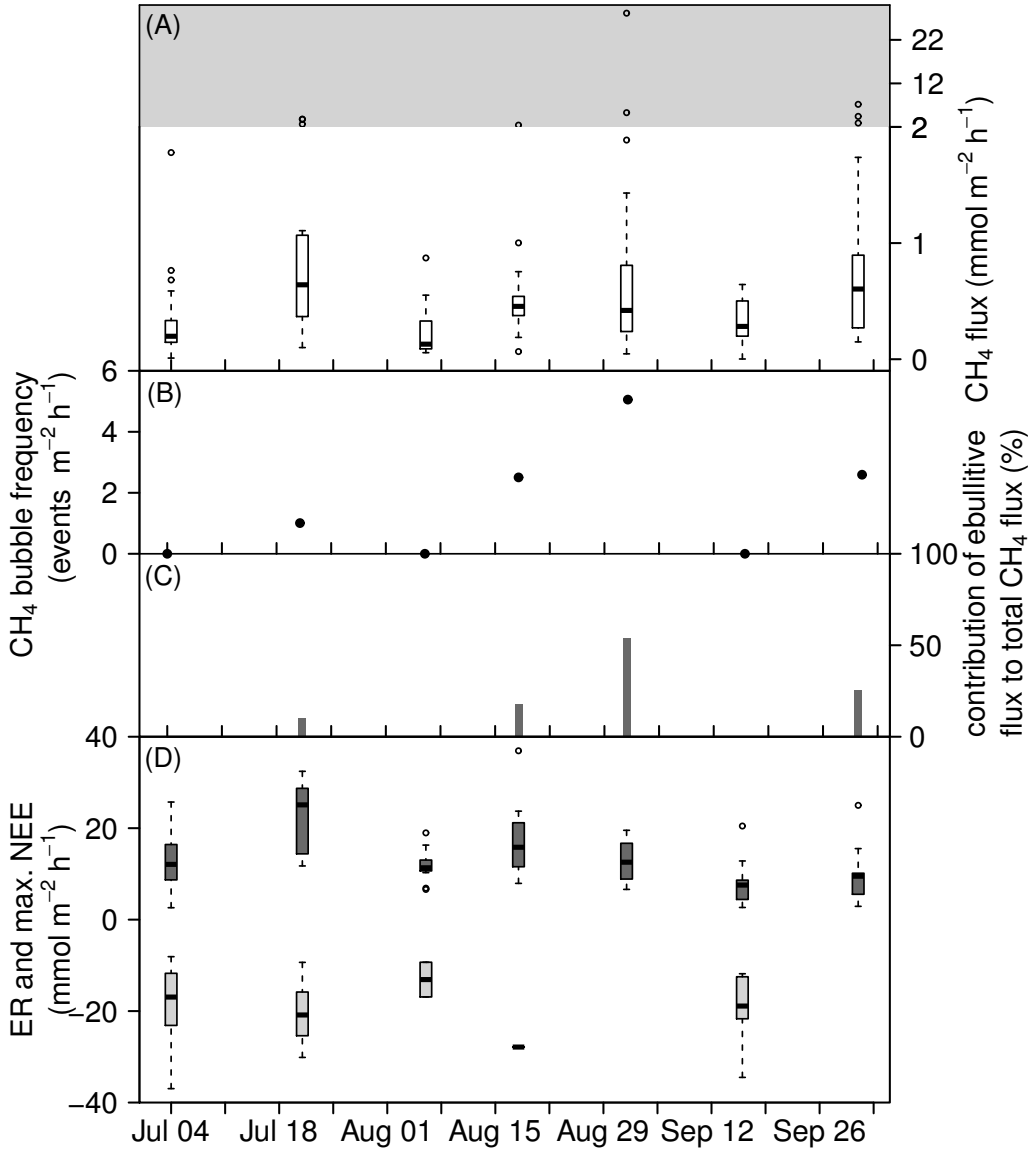


Figure 5: Time series of peatland $CH_4$ fluxes (panel A), $CH_4$ bubble frequency (panel B), contribution of ebullitive $CH_4$ flux to total $CH_4$ flux (panel C) as well as ecosystem respiration (ER) and maximum net ecosystem exchange (NEE) (panel D) on measuring days from July 4$^{th}$ until October 1$^{st}$, 2014. Note the different scaling of the y-axis within the gray area in panel (A). In panel (D), the dark gray boxes show the daytime ER and the light gray boxes the maximum net ecosystem exchange at values of photosynthetically active radiation > 1000 µmol $m^{-2}$ $s^{-1}$. In panel (A) and (D), the bold horizontal line shows the median, the bottom and the top of the box the 25$^{th}$ and 75$^{th}$ percentile and the whiskers include all values within 1.5 times the interquartile range.

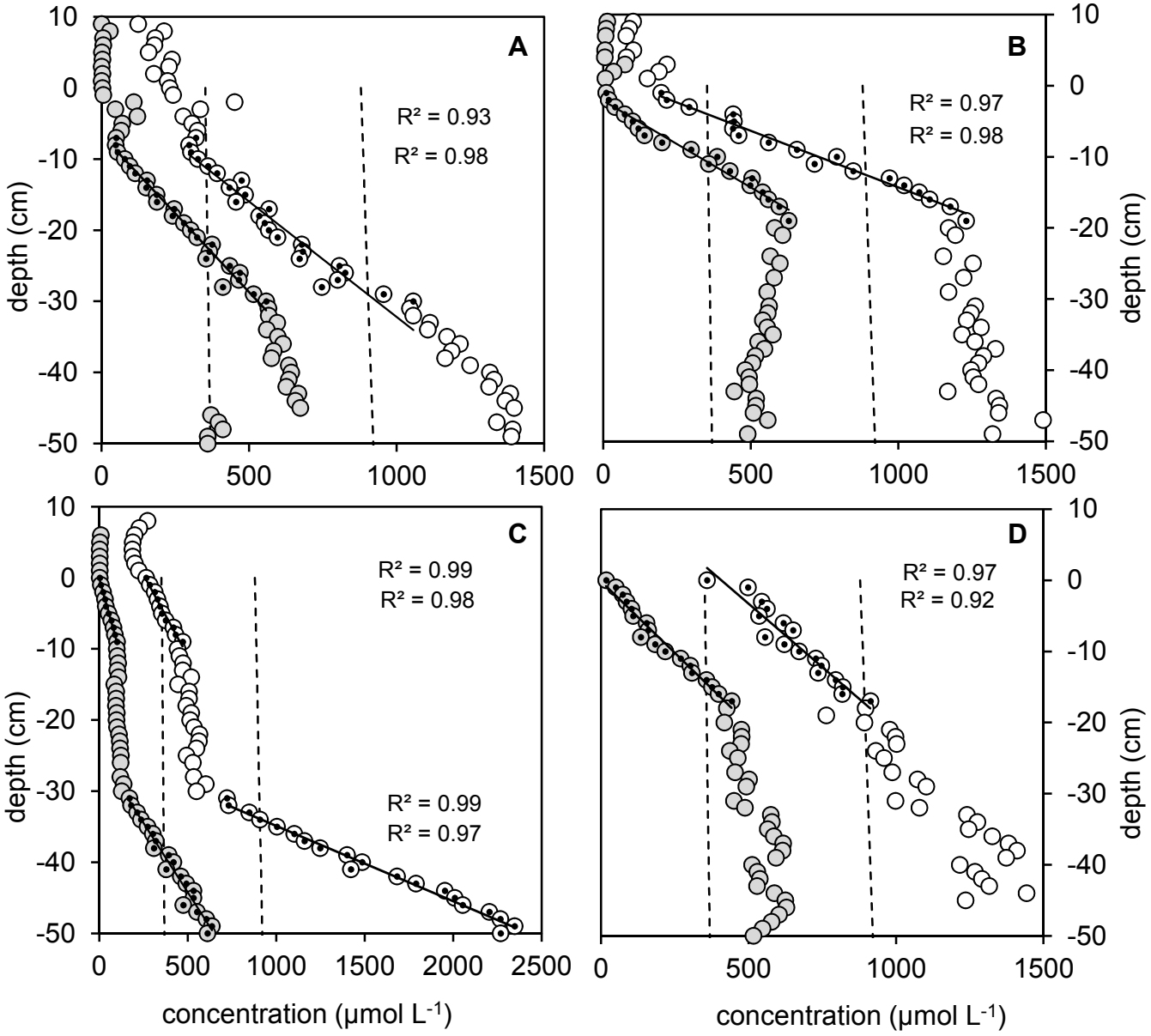


Figure 6: $CH_4$ (shaded symbols) and $CO_2$ (open symbols) concentrations near the sediment-water interface and in the sediment of the pond in four locations (A – D) on September 25th and 29th, respectively, as obtained with porewater peepers. Water depth at the locations was about 0.5 meters; a depth of zero on the y-axis indicates the assumed sediment-water interface. Black lines represent regression slopes (with regression coefficient $R^2$) used to calculate diffusive fluxes towards the sediment-water interface. Dashed lines denote depth and temperature dependent theoretical thresholds for formation of $CH_4$ bubbles at 0.8 atm (lower line) and 0.5 atm (upper line) partial pressure of $N_2$ in the pond sediment at 15°C. In panel C also the diffusive flow from deeper sediment layers was calculated.

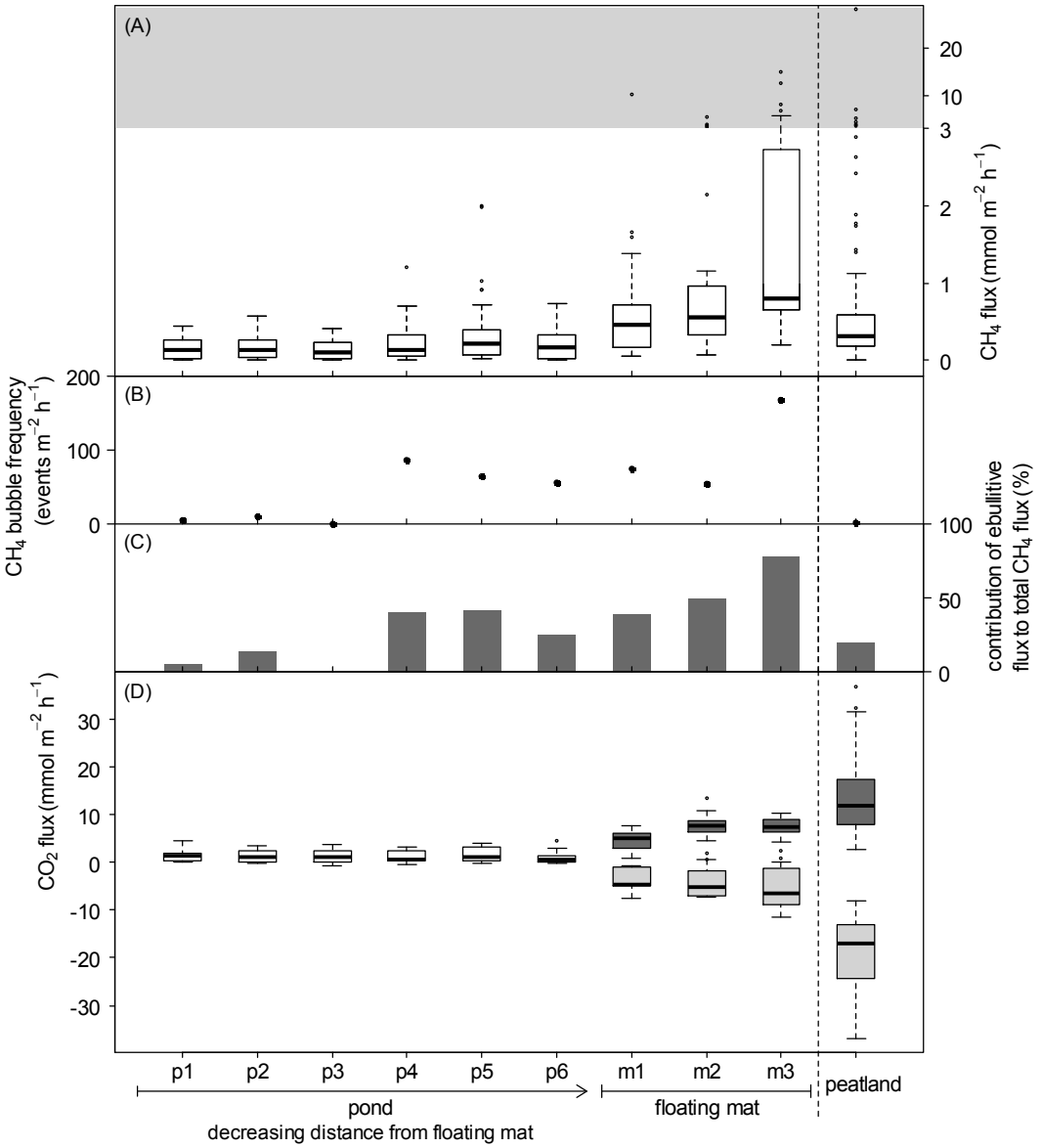


Figure 7: $CH_4$ fluxes (panel A), $CH_4$ bubble frequency (panel B), contribution of ebullitive $CH_4$ flux to total $CH_4$ flux (panel C) and $CO_2$ fluxes (panel D) of the pond (p1 to p6) along a gradient of decreasing distance from the floating mat, of the 3 measuring plots on the floating mat (m1 to m3) and of the peatland site for comparison. Note the different scaling of the y-axis within the gray area in panel (A). In panel (D), the transparent boxes show the net $CO_2$ flux of the pond, the dark gray boxes the daytime ER and the light gray boxes the maximum net ecosystem exchange of the floating mat and the peatland at values of photosynthetically active radiation > 1000 µmol $m^{-2}$ $s^{-1}$. In panel (A) and (D), the bold horizontal line shows the median, the bottom and the top of the box the 25$^{th}$ and 75$^{th}$ percentile and the whiskers include all values within 1.5 times the interquartile range.

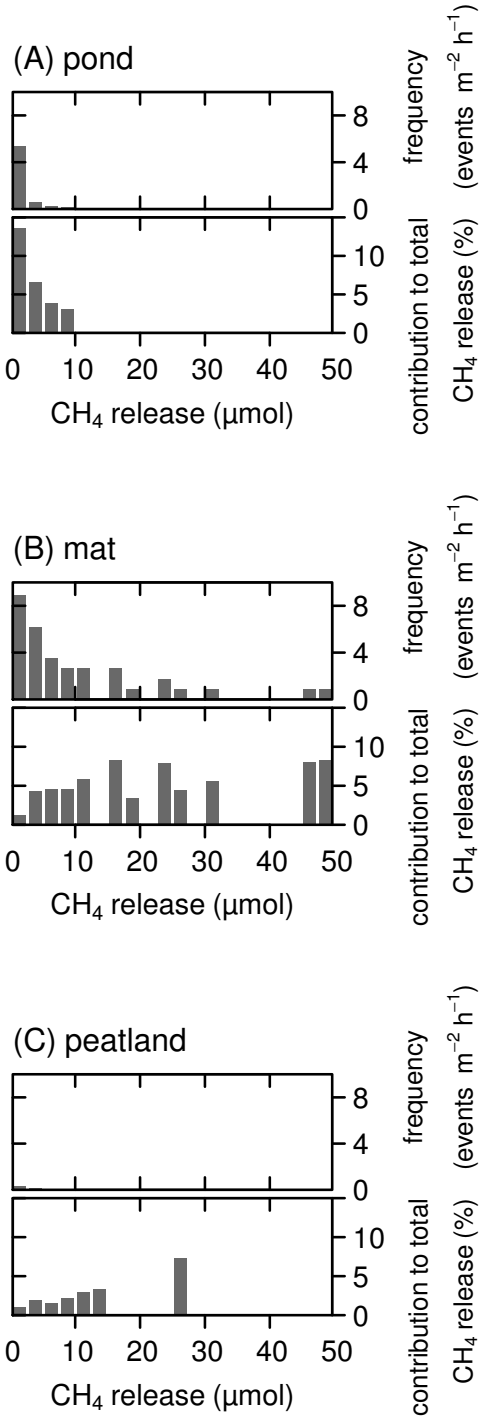


Figure 8: Frequency distribution of ebullitive $CH_4$ release (upper panels) as well as contribution of each size group of ebullitive $CH_4$ release to the total $CH_4$ release (lower panels) of the pond (panel A), the floating mat (panel B) and the peatland (panel C).

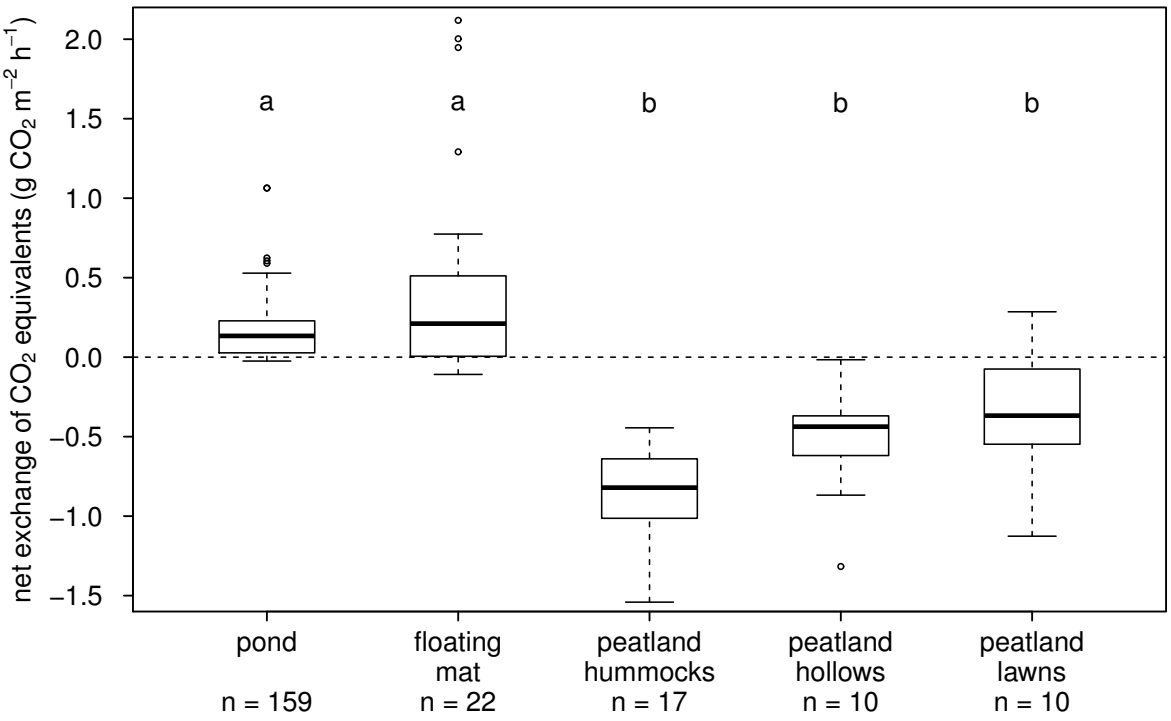


Figure 9: Daytime net exchange of $CO_2$ equivalents of the pond, the floating mat and the three different microforms of the peatland. Different letters indicate significant differences (Kruskal-Wallis multiple comparison test, $p < 0.001$, $n = 218$). For comparability of the $CO_2$ fluxes of the floating mat and the peatland, only maximum net ecosystem exchange at values of photosynthetically active radiation > 1000 µmol $m^{-2}$ $s^{-1}$ was used for the calculation. The bold horizontal line shows the median, the bottom and the top of the box the 25$^{th}$ and 75$^{th}$ percentile and the whiskers include all values within 1.5 times the interquartile range.